Oxidation-driven surface dynamics on NiAl(100)

Hailang Qin[a], Xidong Chen[b], Liang Li[a], Peter W. Sutter[c], and Guangwen Zhou[a,1]

[a]Department of Mechanical Engineering & Multidisciplinary Program in Materials Science and Engineering, State University of New York, Binghamton, NY 13902; [b]Department of Chemistry, Physics and Engineering, Biola University, La Mirada, CA 90639; and [c]Center for Functional Nanomaterials, Brookhaven National Laboratory, Upton, NY 11973

Edited by Alexis T. Bell, University of California, Berkeley, CA, and approved December 5, 2014 (received for review October 31, 2014)

Atomic steps, a defect common to all crystal surfaces, can play an important role in many physical and chemical processes. However, attempts to predict surface dynamics under nonequilibrium conditions are usually frustrated by poor knowledge of the atomic processes of surface motion arising from mass transport from/to surface steps. Using low-energy electron microscopy that spatially and temporally resolves oxide film growth during the oxidation of NiAl(100) we demonstrate that surface steps are impermeable to oxide film growth. The advancement of the oxide occurs exclusively on the same terrace and requires the coordinated migration of surface steps. The resulting piling up of surface steps ahead of the oxide growth front progressively impedes the oxide growth. This process is reversed during oxide decomposition. The migration of the substrate steps is found to be a surface-step version of the well-known Hele-Shaw problem, governed by detachment (attachment) of Al atoms at step edges induced by the oxide growth (decomposition). By comparing with the oxidation of NiAl(110) that exhibits unimpeded oxide film growth over substrate steps we suggest that whenever steps are the source of atoms used for oxide growth they limit the oxidation process; when atoms are supplied from the bulk, the oxidation rate is not limited by the motion of surface steps.

oxidation | NiAl | surface steps

Surface growth processes are often treated with a simplifying assumption that the substrate is immobile. The rationale behind this general belief is that the role of the rigid substrate is to serve as a structural template, guiding the arrangement of impinging atoms. However, many surface growth processes involve reaction with the substrate (i.e., require sources or sinks of substrate atoms). In such cases, the role of the metallic substrate goes far beyond that of a passive support because of its active participation in the growth process. Such surface growth processes are typified by the oxidation of metals, during which the interaction between oxygen and a metallic substrate results in oxide growth by consuming the substrate atoms. Although extensive interest in understanding surface oxidation has existed for decades owing to its critical role in many technological processes including high-temperature corrosion, heterogeneous catalysis, and thin film processing, many issues are still unresolved, particularly those concerning the early stages of oxidation. A detailed understanding of the initial oxidation processes of surfaces has always been complicated by overwhelming inhomogeneities owing to high density of defects. Atomic steps are present on virtually any crystalline material in any environment and serve as natural sources and sinks of substrate atoms owing to the reduced coordination of atoms at step sites. In this work we address oxidation-induced surface dynamics as a result of mass transfer from and to steps. This is a critical issue because it influences both the mechanism and kinetics of the surface physical and chemical processes that involve active participation of substrate atoms, such as oxidation, silicidation, and nitridation, among others.

NiAl is an ordered intermetallic material possessing a high melting point, low density, good oxidation and corrosion resistance, and metal-like electrical and thermal conductivities. These properties make NiAl an attractive material for high-temperature applications such as gas turbine engines. Understanding the initial oxidation of NiAl alloys is important to gain better insight into the oxide film growth and alloy degradation. Besides this technological importance, NiAl is also a prototype system for studying oxidation of intermetallics, composed of a component (Al) that is preferentially oxidized whereas the other (Ni) does not participate in the reaction with oxygen. Low-energy electron microscopy (LEEM), capable of imaging surfaces in video rate during gas exposure and at elevated temperatures, has been used to visualize the initial oxidation of NiAl(110), revealing the formation of aluminum oxide stripes that can elongate from one substrate terrace to the next by overgrowing surface steps (1–3). A similar stripe morphology of aluminum oxide has also been observed in NiAl(100) oxidation, although a detailed explanation of the mechanisms of the oxide growth is lacking (4–11). Here, we use in situ LEEM observations of the initial-stage oxidation of NiAl(100) at elevated temperatures to quantitatively relate the Al_2O_3 growth to the mass transfer process on the NiAl(100) surface. The growth of Al_2O_3 stripes during the oxidation of the NiAl(100) surface involves the supply of Al adatoms from substrate steps. By analyzing oxide stripe growth and the displacement of step edges we show that both ascendant and descendant steps represent sources of Al atoms for oxide growth. At the same time, substrate steps are impermeable to oxide growth. As a result, steps are pushed into bunches by the advancing oxide stripes, and this step bunching retards step motion and thereby reduces the supply of Al adatoms, which slows down and eventually stops the oxide growth. The mass transfer from substrate steps to the oxide is reversed during oxide decomposition, which results in the debunching of steps piled in front of oxide stripes. We establish a connection of the motion of substrate steps with the well-known Hele-Shaw problem of fluid mechanics. A solution for a drain of step atoms is obtained through conformal mapping for fundamental understanding of the fluid-like reaction dynamics at solid surfaces.

Significance

Oxidation of metals involves the reaction of oxygen with the metallic substrate, requiring sources or sinks of substrate atoms. This study provides direct evidence that atomic steps serve as the sources of Al surface atoms for aluminum oxide growth in the oxidation of NiAl(100), which results in coordinated migration and bunching of steps that progressively impedes the oxide growth. Comparison with the oxidation of NiAl(110) that exhibits unimpeded oxide film growth over substrate steps suggests that whenever steps are the source of atoms used for oxide growth they limit the oxidation process; when atoms are supplied from the bulk, the oxidation rate is not limited by the motion of surface steps.

Author contributions: G.Z. designed research; H.Q., X.C., L.L., and P.W.S. performed research; P.W.S. contributed new reagents/analytic tools; H.Q., X.C., and G.Z. analyzed data; and H.Q., X.C., P.W.S., and G.Z. wrote the paper.

The authors declare no conflict of interest.

This article is a PNAS Direct Submission.

Freely available online through the PNAS open access option.

[1]To whom correspondence should be addressed. Email: gzhou@binghamton.edu.

This article contains supporting information online at www.pnas.org/lookup/suppl/doi:10.1073/pnas.1420690112/-/DCSupplemental.

A comparison with the oxidation of NiAl(110) suggests that a transition in the source of Al adatoms from surface steps [for NiAl(100)] to the bulk [for NiAl(110)] promotes the overgrowth of the oxide across steps and thus eliminates the effect of steps on the oxidation process.

Results and Discussion

Fig. 1 shows a sequence of in situ LEEM images (captured from Movie S1) revealing the nucleation and growth of alumina stripes while exposing a clean NiAl(100) surface at 868 °C to 5×10^{-10} torr of oxygen in the first ∼200 s and thereafter $\sim 6 \times 10^{-10}$ torr. As seen in the LEEM image in Fig. 1*A*, the surface has a step-terrace morphology, where dark lines show the locations of atomic steps on the NiAl substrate and the center area has well-separated steps. After a few seconds of oxygen exposure, oxide islands exclusively nucleate at step edges and then develop into elongated stripes. A remarkable growth feature is revealed in Fig. 1 *A*–*D*: The oxide stripes do not cross over substrate steps; instead, surface steps migrate in tandem with the advancement of the oxide stripes. This is evident by observing the growth of two oxide stripes indicated by A and B. The two oxide islands nucleate nearly at the same location and grow on the same terrace but in opposite directions, where island A grows toward step 2 whereas island B grows toward step 1. Given the opposite advancement of the two stripes on the same terrace, one of the steps must be ascendant and the other descendant. The terrace supporting the oxide islands widens as the oxide stripes grow longer, from ∼1.4 μm (t = 0) to ∼2.3 μm (t = 70 s). The in situ LEEM images also reveal that the oxide stripes grow via an adatom mechanism (i.e., Al and O adatoms diffuse in across the terrace and add onto the oxide growth front). The observed step motion implies that surface steps act as sources for Al adatoms that react with oxygen to form oxide stripes. As the oxide stripes lengthen, both steps 1 and 2 become highly curved toward the advancement direction of the stripes. Note that step 3 is a screw dislocation that is initially bounded with step 1 and later becomes debounded owing to the advancement of step 1 with the growth of oxide stripe B.

Fig. 1*E* shows the length evolution of oxide stripes A and B as a function of oxidation time, measured from the in situ LEEM movie. In the first ∼200 s, both stripes show a relatively linear growth behavior but stripe B has a smaller growth rate, which is due to the presence of a step edge that stripe B encounters at the beginning of its growth. At t ∼200 s the oxygen pressure is slightly increased to 6×10^{-10} torr and the growth rate of stripe A increases from ∼5 nm•s^{-1} to ∼10 nm•s^{-1}, whereas the growth of stripe B increases from ∼1.3 nm•s^{-1} to about ∼15 nm•s^{-1}, as extracted from linear fits to the data. The growth of stripe A slows down slightly after ∼300 s; this slowing coincides with an increased number of surface steps piled up in front of the oxide growth front.

Fig. 2 illustrates a sequence of in situ LEEM images (captured from Movie S2) demonstrating that descendant steps can also be sources of Al adatoms for oxide growth if ascendant steps are absent on the terrace (note that the LEEM observation shown in Fig. 2 was made on the same surface region as shown in Fig. 1). Fig. 2*A* shows that the surface has already developed some alumina stripes formed during the oxidation stage shown in Fig. 1. We focus on the migration of the three steps marked by 1, 2, and 3 during the growth of oxide stripe A (Fig. 2*A*) and stripe B that appears at a later time (Fig. 2 *C* and *D*). As seen in Fig. 2*A*, a thin alumina stripe (A) starts from the side of an existing coarsened oxide stripe and grows toward the well-separated steps 1, 2, and 3. When the thin stripe reaches step 1, it pushes the step to advance jointly with it (Fig. 2*B*). As the oxide stripe extends further, it reaches step 2 and now pushes both steps 1 and 2 (Fig. 2 *B* and *C*). As a result, steps 1 and 2 are piled up in front of stripe A. By comparing Fig. 2 *A* and *C* one notes that the terrace width between steps 1 and 2 decreases significantly owing to the step bunching at the leading front of the oxide stripe. Measurements made from the in situ LEEM movie on the length evolution of oxide stripe A as a function of oxidation time are plotted in Fig. 2*E*. The data reveal that the oxide stripe initially grows at a constant rate on the step-free terrace. When encountering step 1 (marked by the arrow in Fig. 2*E*) its growth rate decreases significantly, from 299 nm•s^{-1} to 15 nm•s^{-1}. When it impinges on step 2, the growth rate decreases further to ∼10 nm•s^{-1}, as

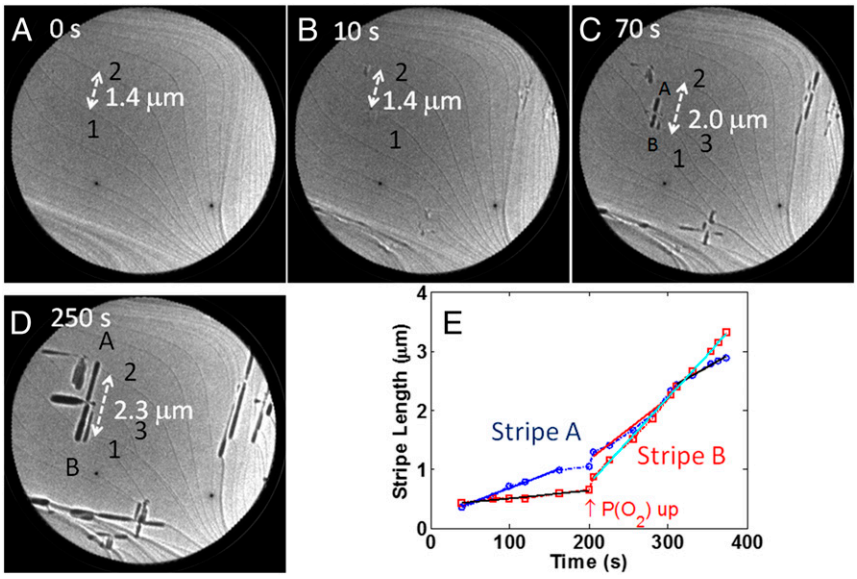

Fig. 1. (*A*–*D*) Time sequence of LEEM images (in situ LEEM Movie S1, image size 10 × 10 μm) of the nucleation and growth of aluminum oxide stripes on a stepped NiAl(100) surface at 868 °C and $pO_2 = 5 \times 10^{-10}$ torr in the first ∼200 s and $pO_2 = 6 \times 10^{-10}$ torr thereafter. The oxide islands nucleate at step edges and grow in tandem with the propagation of the surface steps of the NiAl substrate. (*E*) Dependence of the growth length of oxide stripes A and B on oxidation time measured from the in situ LEEM video.

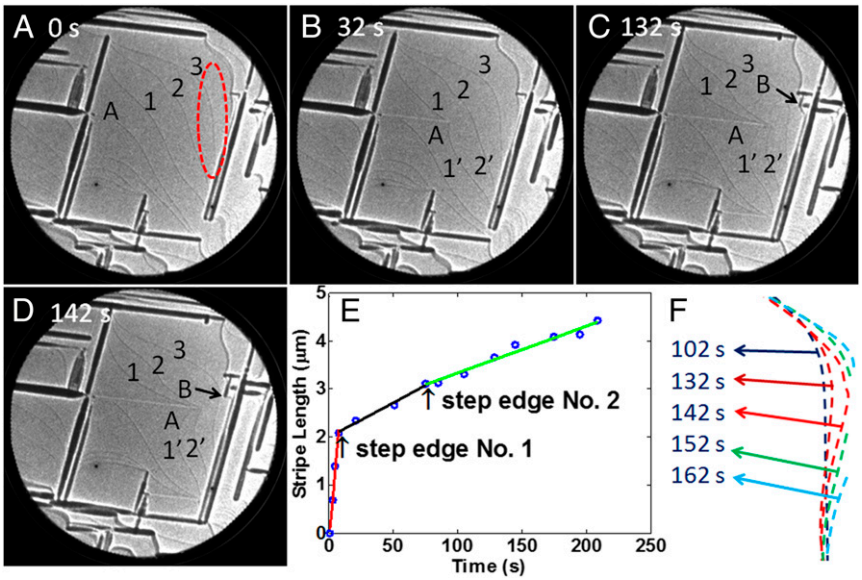

Fig. 2. (*A–D*) Time sequence of LEEM images (in situ LEEM Movie S2, image size 10 × 10 μm) visualizing the migration of substrate steps as the oxide stripes grow on NiAl(100) at 868 °C and $pO_2 = 5 \times 10^{-10}$ torr. (*E*) Dependence of the growth length of oxide stripe A on oxidation time measured from the in situ LEEM video. (*F*) Traces of the position of step 3 at different times show that the step moved toward the growing oxide stripe of B.

extracted from the linear fit. Whereas the oxide stripe continues to advance at a slower rate after impinging on substrate steps and pushing the steps to advance jointly, stripe A completely stops its growth once it reaches a perpendicular oxide stripe (Movie S2).

Fig. 2*C* shows the formation of a new oxide stripe (B) at the upper right corner near step 3. As stripe B grows, the adjacent step 3 moves rapidly toward stripe B and attaches to the side of stripe B. Detailed tracing of the movement of step edge 3 is shown in Fig. 2*F*, where the positions of the step edge at different times are shown together for comparison. The analysis clearly shows that step 3 moves progressively toward the oxide stripe B. For the growth of stripe B, step 3 is the nearest source of Al atoms. From this tracing one can infer that step 3 is descendant from the terrace on which stripe 3 grows (i.e., it recedes toward the terrace as it releases Al atoms). Hence, all of the steps 1, 2, and 3 are ascendant steps for the growth of stripe A, whereas they are descendant steps for stripe B. That is to say, stripe A grows on the bottom terrace whereas stripe B grows on the top terrace. After clarifying the step geometry it becomes obvious that Al adatoms detached from step 3 can climb from the lower to the upper terrace on which oxide stripe B grows. Because there are no ascendant steps available for the terrace on which stripe B grows, the descendant steps become the only source of Al for oxide growth.

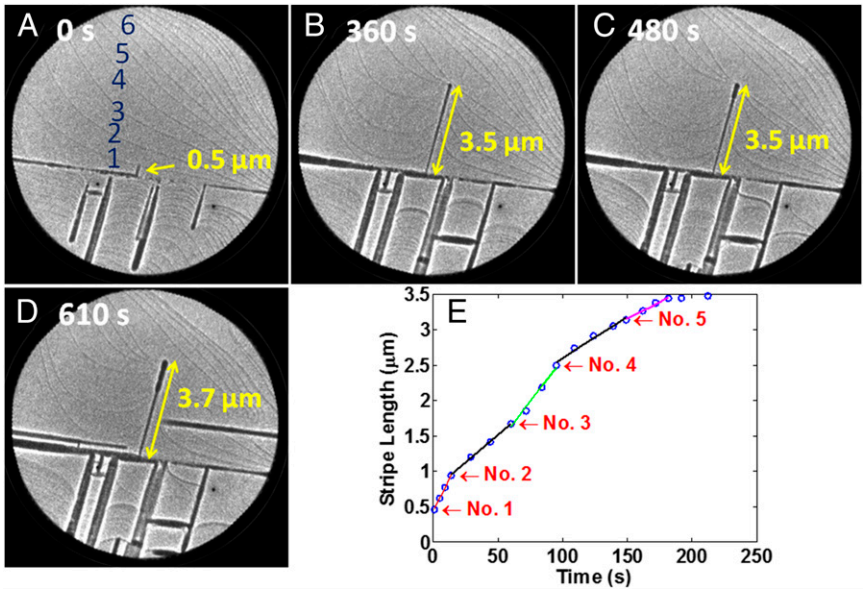

Fig. 3. (*A–D*) Time sequence of LEEM images (in situ LEEM Movie S3, image size 10 × 10 μm) of the advancement of an oxide strip as it encounters multiple substrate steps in the course of its growth on NiAl(100) at 844 °C and pO_2 of 4.7×10^{-10} torr (0 s to 503 s) to around 6.6×10^{-10} torr (after around 503 s). (*E*) Dependence of the growth length of the oxide stripe on oxidation time measured from the in situ LEEM video.

Fig. 3 *A–E* presents a sequence of in situ LEEM images (captured from Movie S3) of the growth of a single oxide stripe in a portion of the NiAl(100) substrate with a relatively high step density. It can be seen from Fig. 3*A* that the stripe starts from the edge of an existing oxide stripe and encounters several steps in the course of its advancement. Similar to what is observed in Figs. 1 and 2, the oxide stripe pushes each substrate step that it encounters to advance jointly with the step edge in its path, which results in the bunching of a growing number of steps in front of the oxide stripe. Fig. 3*F* shows the measured length evolution of the oxide stripe as a function of oxidation time, where the number of steps indicated on the plot is correlated with the moments at which the oxide stripe encounters the respective surface steps. For the first several encounters with steps there is no obvious change in the growth rate. As more steps are piled up at the leading edge, the advancement of the oxide stripe slows down dramatically and then stops. The phenomenon that an oxide stripe continues its advancement after encountering a few steps and then stops completely after encountering more step edges is often observed in different sample regions.

Step bunching can affect oxide growth in two ways: by limiting the supply of Al from the step and by preventing the further advance of the oxide growth front. This is supported by observations showing that if sufficient Al is available from nearby steps the oxide may continue growing even in the presence of a step bunch preventing its further advance (i.e., by expanding laterally or backward). Fig. 3 *B–D* show a situation in which the growth along the long axis of the oxide stripe is pinned owing to a pileup of steps in front of the oxide stripe. At t ~480 s (Fig. 3*C*) the oxide stripe starts to grow in width and the laterally wider section propagates backward along the stripe. The length of the stripe remains fixed at 3.5 μm, the same as at 360 s (Fig. 3*B*). At ~503 s the oxygen pressure is slightly increased to 6.6×10^{-10} torr and the oxide stripe accelerates its growth in the backward direction. The increased oxygen chemical potential also drives the renewed growth forward, from 3.5 μm to 3.7 μm at ~610 s. This relengthening of the stripe is accompanied by additional movement of the bunched steps in front of the stripe (i.e., additional detachment of Al atoms from these step edges is correlated with the increased oxygen pressure). The coordinated migration of the piled steps suggests that the leading edge of the oxide stripe does not reach the downward edge of the steps piled ahead; therefore, Al atoms can still detach from the bunched steps to support the oxide growth once additional oxygen atoms are available (i.e., the increase in oxygen pressure shown above).

In view of the low oxygen gas pressure in our oxidation experiments and oxygen pressure-dependent oxide growth shown in Figs. 1 and 3, we make the assumption that the oxide growth is limited by surface diffusion of adsorbed oxygen atoms to the oxide stripe. Because the oxidation reaction occurs at the leading edge of the stripe, the linear growth rate of the oxide stripe can be expressed as

$$\frac{dx}{dt} = \frac{F}{Nw}, \qquad [1]$$

where x is the length of the oxide stripe, F the surface flux of oxygen atoms, N the number of oxygen atoms incorporated into a unit volume of the oxide layer, and w the width of the stripe. The flux F is given by $F = k(C_0 - C^*)$, where k is the oxygen surface diffusion coefficient, C_0 the average concentration of oxygen absorbed on the metal surface, and C^* the average concentration of oxygen at the reaction site of the oxide stripe, which is the growth front of the oxide stripe. C_0 is a constant that depends on temperature and oxygen pressure. Once a steady state of growth has been reached, C^* is constant as well. Therefore, Eq. **1** gives rise to a linear growth behavior (i.e., constant growth rate) for constant temperature and oxygen pressure, which agrees well with the behavior shown in Figs. 1–3. According to Langmuir absorption theory (12), the concentration of the absorbed oxygen C_0 is proportional to pressure at low gas pressures. Hence, increasing the oxygen pressure increases the oxide growth rate, which is also what we observe (Fig. 1).

Oxygen that has been absorbed on a metal surface may be reevaporated into the gas phase. Previous studies indicate that the ratio of the surface diffusion barrier and the evaporation barrier is between 1/5 and 1/40 (13). The possibility of reevaporation implies the existence of an oxygen capture zone near the oxide growth front; oxygen that lands within this zone can diffuse and reach the reaction site before desorbing into the gas phase. Based on Brownian motion, the radius l of this oxygen capture zone is related to the difference between the diffusion barrier and the evaporation barrier as $l/a = \exp(|\Delta E|/2k_BT)$, where a is the distance of a diffusion jump, ΔE the difference between the diffusion barrier and the evaporation barrier, k_B the Boltzmann constant, and T temperature. The presence of substrate steps on the surface complicates the growth of oxide stripes on a terrace. Owing to the presence of step-edge barriers (13), oxygen atoms on the terraces above or below the one supporting the oxide stripe cannot participate in the oxide growth as effectively as oxygen adsorbed on that terrace itself. Hence, when the growth front of an oxide stripe approaches a step edge to a distance smaller than the above reaction radius l the growth will be slowed down. This is what we observed in our experiment as shown in Figs. 1 and 3, where the oxide stripe growth slows down or completely stops after multiple steps are piled up in front of the oxide stripe. The oxygen surface diffusion-limited oxide growth observed here is also in accordance with the oxide growth on NiAl(110) (1), although the sources of Al surface adatoms for the oxide growth are completely different between the NiAl(100) and NiAl(110) surfaces, as discussed later.

Because the consumption of Al atoms will increase with oxygen pressure we can test the ability of the surface steps to

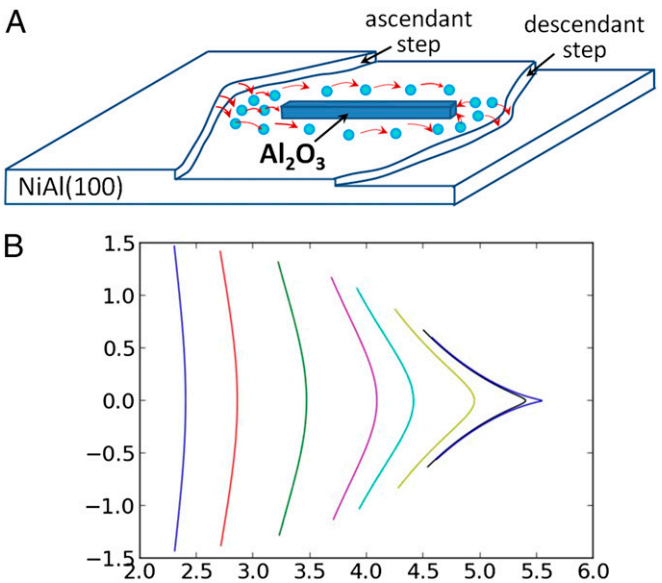

Fig. 4. (*A*) Pictorial illustration of the oxide growth induced migration of substrate steps in front of an oxide stripe, where the steps are ascendant and descendant with respect to the growth directions of the oxide stripe at its two ends. (*B*) An exact solution of the Hele-Shaw moving boundary problem for a single drain shows the evolution of a step edge. The x and y coordinates are scaled by the lattice spacing. A cusp is being formed as time goes by. This behavior agrees qualitatively with our experimentally observed shape evolution of substrate steps.

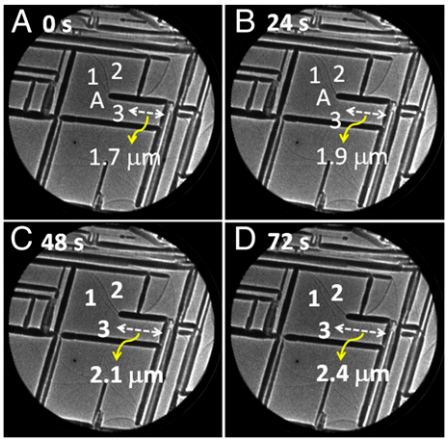

Fig. 5. (*A–D*) Time sequence of LEEM images (in situ LEEM Movie S4, image size 10 × 10 μm) of the decomposition of an oxide stripe as it separate from multiple substrate steps in the course of its decomposition on NiAl(100) at 868 °C after the oxygen supply is shut off.

maintain adequate Al surface adatoms for oxide growth by increasing the dosing oxygen pressure. Single and piled steps are indeed able to keep up with the supply of oxygen adatoms within the range of the oxygen pressures examined, as shown in Figs. 1–3, where the contour evolution of the substrate steps is due to the attachment and detachment of Al atoms. However, if sufficient steps are bunched together in front of the oxide stripe, they are bound to stop the advancement of the oxide stripe at some point because the cost of the energy of creating the new length of the piled steps can exceed the gain due to the formation of the oxide. Because Al atoms are incorporated into the oxide at the front of the oxide stripe, the Al concentration is lower at this growth front than at the substrate step in front of the oxide stripe. This causes local chemical potential variations. The chemical potential differences lead to a mass flow and the net mass flux j can be expressed as $j = -D_S \nabla \mu$, where μ is the local chemical potential and D_S is the surface diffusivity of Al (14). Because the step motion can be considered as an incompressible flow, the velocity potential ϕ then satisfies the Laplace equation, $\nabla^2 \phi = 0$. The boundary condition at the step edge is simply $v_n = \partial\phi/\partial n$, where v_n is the component of the velocity of the motion of the substrate step that is normal to the step boundary and $\partial\phi/\partial n$ is the directional derivative of the velocity potential along the normal direction.

The framework described above clearly qualifies step motion as a moving boundary problem. A mathematically identical problem called the Hele-Shaw problem has been studied extensively (15). With conformal mapping a solution for a point drain has been obtained (16), which can be used to describe the motion of surface steps observed in our experiments. The oxide growth front serves as a sink of Al adatoms detached from step edges. As revealed from the LEEM observations shown in Figs. 1 and 2, the oxide stripe growth is accompanied by the coordinated migration of substrate steps (i.e., the surface step advances locally in the growth direction of the oxide stripe regardless if the step is ascendant or descendant, as shown schematically in Fig. 4*A*). For an ascendant step with respect to the oxide growth direction, the incorporation of Al atoms from the step results in the retraction of the surface step in front of the oxide stripe. In the case of a descendant step, Al adatoms diffuse across the terrace and attach to both the oxide and the descendant step ahead of its growth front, which results in the coordinated advancement of both the oxide stripe and the step in the same direction. Because our mathematical model only focuses on the moving boundary, it actually describes both of the two cases, which share the same solution. The following mapping function can be used to obtain an exact solution of the governing equation of the step migration induced by local chemical potential difference, $z = -\log\varsigma + b(t) + d(t)\varsigma$, where z is a complex variable that describes the moving step, ζ gives a half circle on another complex plane, which defines a conformal map that maps the initial straight step boundary, and $b(t)$ and $d(t)$ are both a function of time. The initial conditions are $b(0) = 0$, $d(0) = \varepsilon << 1$. ε describes an initial perturbation to the straight step boundary as a growing oxide stripe gets close to a step edge (more detail is given in supplementary information). The above exact solution is plotted in Fig. 4*B*, which reproduces the shape evolution of surface steps observed in Figs. 1–3.

Slightly decreasing the oxygen pressure can lead to decomposition of the oxide stripes, which results in debunching of the steps piled up in front of them. Fig. 5 illustrates a sequence of in situ LEEM images (captured from Movie S4) of the migration of substrate steps during the decomposition of an oxide stripe, which provide further insight into the mass transport process. As seen in Fig. 5*A*, steps 1 and 2 are piled up ahead of the growth front of an oxide stripe (marked A), whereas step 3 projects toward the side of the stripe. As the oxide decomposes step 3 moves to the left and its distance to the oxide stripe behind increases from ~1.7 μm (Fig. 5*A*) to 2.4 μm (Fig. 5*D*). As seen in Fig. 5*C*, steps 1 and 3 actually are segments of the same step, as revealed during shrinking of the oxide stripe; this indicates that the growth front of stripe A is originally wrapped by steps 1 and 3. The process can be described as the release and diffusion of Al atoms from the oxide and their reattachment to the step edges. Al atoms released from oxide stripe A are incorporated into the substrate steps (i.e., the step edges now become sinks of Al atoms released by decomposition of the oxide), which results in the advancement of substrate steps. The other oxide stripes on the surface show no noticeable changes in size, implying that the migration of steps 1 and 2 is mainly due to the attachment of Al released from the decomposition of stripe A. Note that the LEEM observation shown in Fig. 5 is made on the same area as shown in Figs. 1 and 2, and we have already known that steps 1 and 3 are on the lower terrace and step 2 and oxide stripe A are on the upper terrace. The migration of steps 1 and 3 to the left involves downward diffusion of Al atoms released from the oxide stripe.

The in situ LEEM observations described above demonstrate that oxide growth involves massive mass transfer from substrate steps to the oxide as the oxide grows, and vice versa as the oxide decomposes. A unique feature of the oxide growth process is that the oxide stripes do not cross substrate steps. This frustrated step crossing forces the oxide stripe to stay on a single substrate terrace, which leads to the coordinated migration of substrate steps and step bunching as the oxide stripe advances and encounters surface steps (either ascendant or descendant) in the

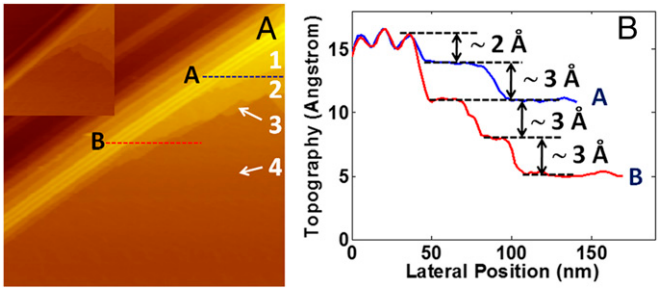

Fig. 6. (*A*) The STM image (size 500 × 500 nm^2, V_{Bias} = −1 V, I_{Tunnel} = 1 nA) shows that the oxide stripe growing from a upper terrace stays on the same terrace even after encountering multiple step edges, instead of crossing the step edges. (*Inset*) An overview of the area (size: 750 × 750 nm^2, V_{Bias} = −1 V, I_{Tunnel} = 1 nA). (*B*) The two STM line profiles correspond to the two dotted lines drawn in *A*.

course of its growth. This growth feature is corroborated by STM imaging as shown in Fig. 6(a). Overview scanning tunneling microscope (STM) images (Fig. 6*A*, *Inset*) show a similar morphology as observed by LEEM (i.e., steps encountered by the stripe all project toward the side of the oxide stripe). The line profiles in Fig. 6*B* (along the dotted lines drawn in Fig. 6*A*) show a stripe height of ~2 Å, compared with the step height of ~3 Å, close to the lattice constant of NiAl (2.89 Å). STM also clarifies the origin of the rather broad oxide stripes (up to ~200 nm) observed by LEEM. As shown in Fig. 6, the wide oxide stripe actually consists of multiple narrower stripes, similar to previous results (5). The spacing of these narrow stripes can be as small as 6 Å (i.e., the lateral size of a single unit cell of θ-Al_2O_3) (10).

Our in situ LEEM observations show no Ni clustering or islanding during the oxide growth, suggesting that Ni atoms liberated through oxidation of Al dissolve in the NiAl bulk. Owing to the high temperatures examined in our study, the diffusion of Ni atoms into the bulk is kinetically probable [diffusion coefficient of Ni: 5×10^{-11} cm^2/s at 1,250 K (17), sufficient for an appreciable extent of Ni diffusion into NiAl (18)]. The dissolution of Ni atoms in the bulk should also be thermodynamically favorable because it leads toward more stable Ni-rich phases (e.g., Ni_3Al) (19). This is also in accordance with ab initio calculations showing the oxidation induced dissolution of Ni in the NiAl bulk (20) and with electron spin resonance experiments that directly show the dissolution of Ni (21).

It is instructive to compare our results on the oxidation of Ni(100) to those obtained on NiAl(110). Using in situ LEEM and STM, McCarty and coworkers (1–3) have shown that aluminum oxide stripes formed during oxidation of NiAl(110) can easily overgrow substrate steps. The surface steps are immobile and the oxide grows over steps without inducing step bunching. The observation of stationary substrate steps suggests that the steps are not a major source of Al atoms in the initial oxidation of NiAl(110), that is, the oxide growth involves Al atoms from another source (i.e., the NiAl bulk). Indeed, McCarty and coworkers (22, 23) have shown that mass transport between the NiAl(110) surface and the bulk can be very efficient at elevated temperatures (750–1,000 °C). For clean NiAl(110) in vacuum, surface Al atoms supplied from the bulk attach to steps, thus inducing step migration (22, 23). However, under oxidizing conditions it is thermodynamically more favorable for Al atoms supplied from the bulk to be incorporated in the growing oxide rather than steps. Therefore, the steps are relatively immobile (i.e., no step bunching occurs) and the oxide can overgrow surface steps with continued supply of Al from the bulk. However, in the oxidation of NiAl(100) surface steps are the main source of Al for the growth of alumina stripes, as shown here. Therefore, substrate steps migrate and subsequently pile up in front of the oxide stripes in the course of the oxide growth, and it becomes increasingly energetically and kinetically unfavorable for the oxide film to overgrow the step bunched region as more steps are piled up in front of the leading edge of the oxide stripe.

The difference in the oxide growth behavior in the oxidation of NiAl(100) and (110) can be attributed to the effect of the crystallographic orientation. NiAl(110) has a more open surface structure than NiAl(100), which may facilitate the supply of Al surface adatoms for the oxide growth via the surface-bulk mass transport. For NiAl(100), the more compact surface structure makes surface steps kinetically more favorable as the sources of Al surface adatoms for the oxide growth. To further test this speculation, we perform density-functional theory (DFT) calculations to determine the energy barriers for the step-edge detachment for monoatomic steps on both NiAl(100) and NiAl(110) surfaces. Our DFT results (Fig. S1) indicate that the energy barriers for the step-edge detachment on NiAl(100) are 0.76 eV and 1.52 eV, respectively, for Al-terminated and Ni-terminated step edges, whereas the corresponding values for the NiAl(110) surface are 1.56 eV and 2.30 eV, respectively (more detail is given in *Supporting Information*). The significantly smaller energy barriers for step-edge detachment on NiAl(100) supports well our experimental observations that surface steps are the main sources of Al surface adatoms for the growth of aluminum oxide stripes in NiAl(100) oxidation. By comparing the oxide growth behaviors of NiAl(100) and (110) we can expect that the oxide growth-induced step bunching can be suppressed if the source of Al surface atoms is changed from substrate steps to the bulk. Indeed, no step bunching was observed for the growth of oxide films on NiAl(110) (1–3).

In summary, we have provided direct evidence for the correlation between surface growth and migration of substrate steps as a result of mass transfer from and to steps in the oxidation of NiAl(100). Our in situ LEEM observations demonstrate that substrate steps are impermeable for oxide film growth that results in significant step bunching in the oxide growth front. For the first time, to our knowledge, the surface step motion due to local chemical potential variations is found to bear relevance with the well-known Hele-Shaw problem, which expands our fundamental understanding of the fluid-like dynamics of the surface migration induced by gas–solid reactions. By comparing with the oxidation of NiAl(110) that shows unimpeded oxide growth over substrate steps we expect broader applicability of our results in manipulating the oxide film growth from completely suppressing step overgrowth to promoting step overgrowth by controlling the crystallographic orientation or step-edge configuration that favors the mass transport via step-edge detachment or surface-bulk exchange.

Materials and Methods

A NiAl(100) single crystal, purchased from Princeton Scientific Corp., cut to within 0.1° to the (100) crystallographic orientation and polished to a mirror finish, was used in our experiments. A clean surface was achieved by flashing the crystal several times up to 1,100–1,200 °C. The surface cleanness and order were checked by X-ray photoelectron spectroscopy, low-energy electron diffraction (LEED), and STM imaging. Oxidation was performed by exposing the clean surface at 844–868 °C to high-purity oxygen gas with a partial pressure in the range of 5.0×10^{-10} torr to 2×10^{-9} torr with a base pressure below 4×10^{-10} torr. All of the LEEM imaging was performed in bright field, at an electron energy of 0.1 V, and in real time at the high temperature during the oxygen dosing. LEED was used to verify the formation and structure of the oxide films formed from the in situ oxidation. The LEED patterns of the oxide films indicate a well-ordered (2×1, 1×2) structure (10, 11), which is in accordance with the formation of θ-Al_2O_3 films adopting the Bain epitaxy relationship between the fcc structure of the oxygen-sublattice and bcc structure of the NiAl substrate [i.e., $(001)_{O\text{-sublattice}} \parallel (001)_{NiAl}$ and $[110]_{O\text{-sublattice}} \parallel [001]/[010]_{NiAl}$] (7, 24–26).

ACKNOWLEDGMENTS. This work was supported by US Department of Energy, Office of Basic Energy Sciences, Division of Materials Sciences and Engineering Award DE-FG02-09ER46600. Research was carried out in part at the Center for Functional Nanomaterials, Brookhaven National Laboratory, which is supported by the US Department of Energy, Office of Basic Energy Sciences, under Contract DE-AC02-98CH10886. This work used the computational resources from the Extreme Science and Engineering Discovery Environment, which is supported by National Science Foundation Grant OCI-1053575.

1. Pierce JP, McCarty KF (2005) Self-assembly and dynamics of oxide nanorods on NiAl(110). *Phys Rev B* 71:125428.
2. Pierce JP, Bartelt NC, Stumpf R, McCarty KF (2008) Stability of ultrathin alumina layers on NiAl(110). *Phys Rev B* 77:195438.
3. McCarty KF, Pierce JP, Carter CB (2006) Translation-related domain boundaries form to relieve strain in a thin alumina film on NiAl(110). *Appl Phys Lett* 88:141902.
4. Gabmann P, Franchy R, Ibach H (1993) Preparation of a well ordered aluminum oxide layer on NiAl(001). *J Electron Spectrosc Relat Phenom* 64-65:315–320.
5. Blum R-P, Ahlbehrendt D, Niehus H (1998) Growth of Al_2O_3 stripes in NiAl(001). *Surf Sci* 396(1-3):176–188.
6. Blum R-P, Niehus H (1998) Initial growth of Al_2O_3 on NiAl(001). *Appl Phys, A Mater Sci Process* 66(1):S529–S533.
7. Fremy N, Maurice V, Marcus P (2002) X-ray photoelectron spectroscopy study of thin oxide layers formed on (001)-oriented NiAl single-crystal surfaces. *Surf Interface Anal* 34(1):519–523.
8. Fremy N, Maurice V, Marcus P (2003) Initial stages of growth of alumina on NiAl(001) at 1025 K. *J Am Ceram Soc* 86(4):669–675.

9. Maurice V, Fremy N, Marcus P (2005) Hydroxylation-induced modifications of the Al_2O_3/NiAl(001) surface at low water vapor pressure. *Surf Sci* 581(1):88–104.
10. Qin HL, Zhou GW (2013) The formation of double-row oxide stripes during the initial oxidation of NiAl(100). *J Appl Phys* 114:083513.
11. Qin HL, Sutter P, Zhou GW (2014) The crystallization of amorphous aluminum oxide thin films grown on NiAl(100). *J Am Ceram Soc* 97(9):2762–2769.
12. Hill TL (1987) *An Introduction to Statistical Thermodynamics* (Dover, Mineola, NY).
13. Ehrlich G, Hudda FG (1966) Atomic view of surface self-diffusion: Tungsten on tungsten. *J Chem Phys* 44:1039–1049.
14. Jeong H-C, Williams ED (1999) Steps on surfaces: Experiment and theory. *Surf Sci Rep* 34:171–294.
15. Saffman PG, Taylor G (1958) The penetration of a fluid into a porous medium or Hele-Shaw cell containing a more viscous liquid. *Proc-R Soc Lond, Math Phys Sci* 245(1242): 312–329.
16. Howison SD, Ockendon JR, Lacey AA (1985) Singularity development in moving-boundary problems. *Q J Mech Appl Math* 38(3):343–360.
17. Hancock GF, McDonnell BR (1971) Diffusion in the intermetallic compound NiAl. *Phys Status Solidi* 4(1):143–150.
18. Jaeger RM, Kuhlenbeck H, Freund H-J (1991) Formation of a well-ordered aluminum oxide overlayer by oxidation of NiAl(110). *Surf Sci* 259(3):235–252.
19. Freund H-J (1997) Adsorption of gases on complex solid surfaces. *Angew Chem Int Ed Engl* 36(5):452–475.
20. Finnis MW, Lozovoi AY, Alavi A (2005) The oxidation of NiAl: What can we learn from ab initio calculations? *Annu Rev Mater Res* 35:167–207.
21. Katter UJ, Schlienz H, Beckendorf M, Freund H-J (1993) Electron spin-resonance (ESR) studies of adsorbate dynamics on single crystal surfaces: Possibilities and limitations. *Ber Bunsenges Phys Chem* 97(3):340–352.
22. McCarty KF, Nobel JA, Bartelt NC (2001) Vacancies in solids and the stability of surface morphology. *Nature* 412(6847):622–625.
23. McCarty KF, Nobel JA, Bartelt NC (2005) Surface dynamics dominated by bulk defects: The case of NiAl(110). *Phys Rev B* 71:085421.
24. Gassmann P, Franchy R, Ibach H (1994) Investigations on phase transitions within thin Al_2O_3 layers on NiAl(001) - HREELS on aluminum oxide films. *Surf Sci* 319(1-2):95–109.
25. Stierle A, Formoso V, Comin F, Franchy R (2000) Surface X-ray diffraction study on the initial oxidation of NiAl(100). *Surf Sci* 467(1-3):85–97.
26. Stierle A, Formoso V, Comin F, Schmitz G, Franchy R (2000) Oxidation of NiAl(100) studied with surface sensitive X-ray diffraction. *Physica B* 283(1-3):208–211.